Volume 1 | Number 1 | Jan 2013 | Pages 1–100
PCCP
Physical Chemistry Chemical Physics

Journal Name
Physical Chemistry Chemical Physics
Dynamic Article Links ►

Cite this: DOI: 10.1039/c0xx00000x

www.rsc.org/xxxxxx

ARTICLE TYPE

Self-assembly of NiTPP on Cu(111): a transition from disordered 1D wires to 2D chiral domains.

Shadi Fatayer[1,*,†], Roberto G. A. Veiga[2], Mauricio J. Prieto[1], Eric Perim[1], Richard Landers[1], Roberto H. Miwa[3], Abner de Siervo[1,*]

Received (in XXX, XXX) Xth XXXXXXXXX 20XX, Accepted Xth XXXXXXXXX 20XX
DOI: 10.1039/b000000x

The growth and self-assembling properties of nickel-tetraphenyl porphyrins (NiTPP) on the Cu(111) surface is analysed via scanning tunnelling microscopy (STM), X-ray photoelectron spectroscopy (XPS) and density functional theory (DFT). For low coverage, STM results show that NiTPP molecules diffuse on the terrace until they reach the step edge of the copper surface forming a 1D system with disordered orientation along the step edges. The nucleation process into a 2D superstructure was observed to occur via interaction of molecules attached to the already nucleated 1D structure, reorienting molecules. For monolayer range coverage a 2D nearly-squared self-assembled array with the emergence of chiral domains was observed. XPS results of the Ni $2p_{3/2}$ core levels exhibit a 2.6 eV chemical shift between the mono- and multilayer configuration of NiTPP. DFT calculations show that the observed chemical shifts of Ni $2p_{3/2}$ occur due to interaction of 3d orbitals of Ni with Cu(111) substrate.

Introduction

Understanding supramolecular organization is a key step towards the development of devices from the bottom-up perspective [1]. This approach could lead to the tailoring of different properties in nanostructured material and presents itself as useful for application in different fields, for example, heterogeneous catalysis [2], optoelectronics [3] and spintronics [4,5]. Besides applications on different devices, the elucidation of how porphyrins adsorb and assemble on surfaces is helpful to gain an understanding on how more complex porphirinoid systems behave, such as hemoglobin [6], chlorophyll [7] as well as enzymes [7,8]. Porphyrins also present interesting magnetic properties, due to the interaction of the central metallic atom with the organic frame that enhance some properties, for example, its magnetic signal [9,10], and the possibility of different on-surface chemical reactions [11,12].

[1] Instituto de Física Gleb Wataghin, Universidade Estadual de Campinas, Campinas 13083-859, São Paulo, Brazil
[2] Departamento de Engenharia Metalúrgica e de Materiais, Escola Politécnica, Universidade de São Paulo, São Paulo 05508-010, São Paulo, Brazil
[3] Departamento de Física, Universidade Federal de Uberlandia, Uberlândia 38400-902, Minas Gerais, Brazil

**A. de Siervo, email: asiervo@ifi.unicamp.br; Shadi Fatayer, e-mail: shadikeitaro@gmail.com*

† Present address: IBM Research – Zurich, 8803 Ruschlikon, Switzerland

Structural and electronic studies on different metallotetraphenyl-porphyrins and 2H-tetraphenylporphyrins and the self-assembling properties on different metal substrates have been extensively investigated in recent years [13, 14, 15, 16, 17, 18], but Nickel-tetraphenylporphyrin (NiTPP) was never explored on Cu(111). Also, in most of these studies, the main interest has been on how porphyrins properties relate to different substrates in the monolayer regime and not with respect to the multilayer phase.

In this study, the growth behaviour of NiTPP on the Cu(111) surface for coverage ranging from submonolayer to multilayer was investigated experimentally combining STM and XPS measurements as well as theoretically by performing DFT calculations. All experiments were performed via STM and XPS at room temperature (RT) in UHV. DFT simulations corroborate our findings and provide additional understanding on the molecular conformation, molecule-molecule and molecule-substrate interactions. It is shown by STM that Cu(111) enables the assembly of different kinds of arrays, both in one and two dimensions. The structural properties explored with STM reveal that for a low concentration of molecules, NiTPP arranges itself in a disordered chain structure whereas in monolayer coverage, the achiral molecule rearranges in a 2D chiral structure. STM images also exhibit the conformation of NiTPP in the saddle shape, an observation supported by our DFT simulations. Chemical information obtained via XPS spectra reveal chemical shifts for different elements when compared between mono- and multilayers of NiTPP. DFT results support the nearly-squared lattice assembly and provide evidence for the hybridization between Ni 3d orbitals and the substrate.

Experimental section

All experiments were performed in two connected ultra-high vacuum (UHV) chambers. One chamber was equipped with a STM and the other one with standard cleaning facilities, XPS and a Knudsen cell for molecule sublimation. The pressure in the XPS chamber was in the low 10^{-10} mbar range and in the STM in the middle 10^{-11} mbar range. The STM microscope used was a SPECS Aarhus 150 equipped with a SPECS SPC 260 Controller. The STM measurements were performed in the constant current mode with a W tip cleaned in situ by Ar+ sputtering. All STM images were taken at room temperature (RT), plane corrected and Gaussian smoothed with WsXM [19]. The calibration of measured distances was performed using the Cu-Cu atomic distances of clean Cu(111) as reference. The photons used in XPS were provided by a Mg-K_α anode (with a small Al-K_α contribution due to crosstalk with Al anode) and the photoelectrons were analysed with a SPECS Phoibos 150 hemispherical analyzer with multi channeltron detection. The XPS peak position was calibrated by comparing with the Au 4f peak.
The Cu(111) crystal was prepared with repeated cycles of sputtering with Ar+ ions (1 keV) and annealing (840 K) in UHV. Prior to molecular deposition, XPS, LEED and STM measurements confirm the substrate surface ordering and cleanliness. NiTPP was purchased from Sigma Aldrich (purity >95%) and deposited using a homemade Knudsen cell from a quartz-crucible. To assure high purity, NiTPP was heated and outgassed for 24 hours at 500 K. The calculated coverage of NiTPP on the copper substrate was determined by the decrease in the XPS Cu $2p_{3/2}$ peak area, and supported by STM images.

Computational section

The calculations were performed within the DFT approach, as implemented in the Quantum-Espresso package [20]. The Kohn-Sham orbitals were expanded in a plane-wave basis set, with an energy cutoff of 28 Ry. We made a set of convergence tests, by considering an energy cutoff up to 35 Ry, where we find that our results for the NiTPP/Cu(111) adsorption energy and equilibrium geometry are converged within an accuracy of around 5%. The Cu(111) surface was described by using the slab method, considering three monolayers (MLs) of Cu. The topmost two MLs were allowed to relax (force convergence of 260 meV/nm). To simulate a single NiTPP molecule adsorbed on the Cu(111) surface, we used a large surface unit cell (composed of 270 Cu atoms, with 90 atoms per ML). In this case, the periodic boundary conditions minimized the NiTPP-NiTPP interaction, as the lateral distance between a given NiTPP (adsorbed) molecule and its nearest neighbour image is equal to 2.2 nm. Whereas, to describe the periodic array of NiTPP on the Cu(111), we have considered a monoclinic cell, with 96 atoms (32 per ML), and lattice vectors of 1.35 nm forming an angle of 82°, and a vacuum region of 1.5 nm. The total charge density was obtained using the Γ point. The convergence with respect to the number of k-points was verified considering up to four k-points. The electronic properties were calculated by considering a set of ten k-points. The NiTPP - Cu(111) interaction was calculated by using the self-consistent vdW-DF approach as described in literature [21, 22, 23].

Results and Discussion

NiTPP disordered nanochains formation.

In the NiTPP/Cu(111) system, for submonolayer coverage (0.3 ML) we observed that molecules anchor at the step edges of the substrate. One of the STM images of submonolayer coverages of NiTPP on Cu(111), is shown in Figure 1 A. The rounded spots represent the molecules deposited on the substrate. NiTPP has such an appearance because of the low magnification used for this image size and the response on the STM feedback due to the difference in height at the step edge. At coverage higher than 0.1 ML, NiTPP also presents a mobile phase at room temperature, which is evident by the streaky features in the STM images (bottom of Figure 2A, for example). Due to the Ehrlich-Schwoebel barrier [24], we observe that molecules adsorb in the lower part of the step edges, which are electron rich. This implies that NiTPP act as an electron acceptor at such coverage.

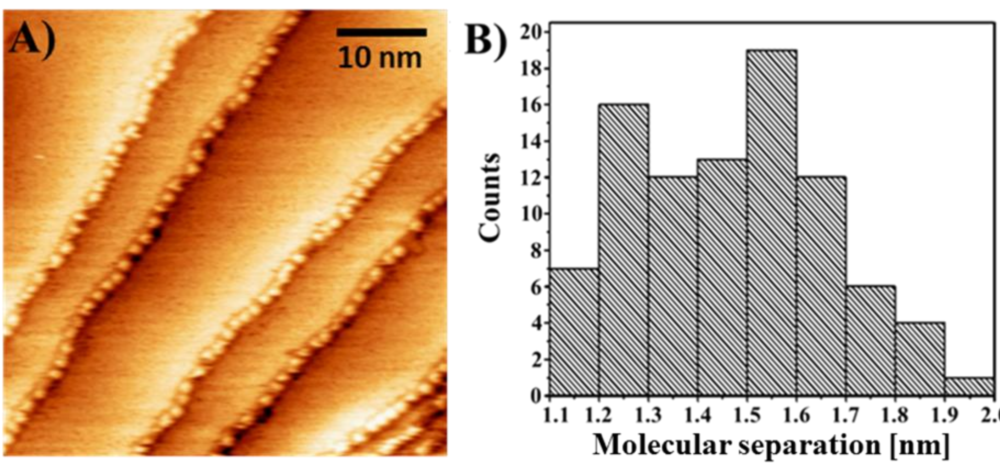

Figure 1. A) STM image (48x48 nm²) showing NiTPP wire formation along the step edges of Cu(111) (VT=1.2 V and IT=0.5 nA). The coverage is lower than 0.1 ML. B) Histogram showing the molecular separation distribution measured parallel to the step edges at a bias voltage of 1.2V. The distribution indicates a disordered alignment relative to the step.

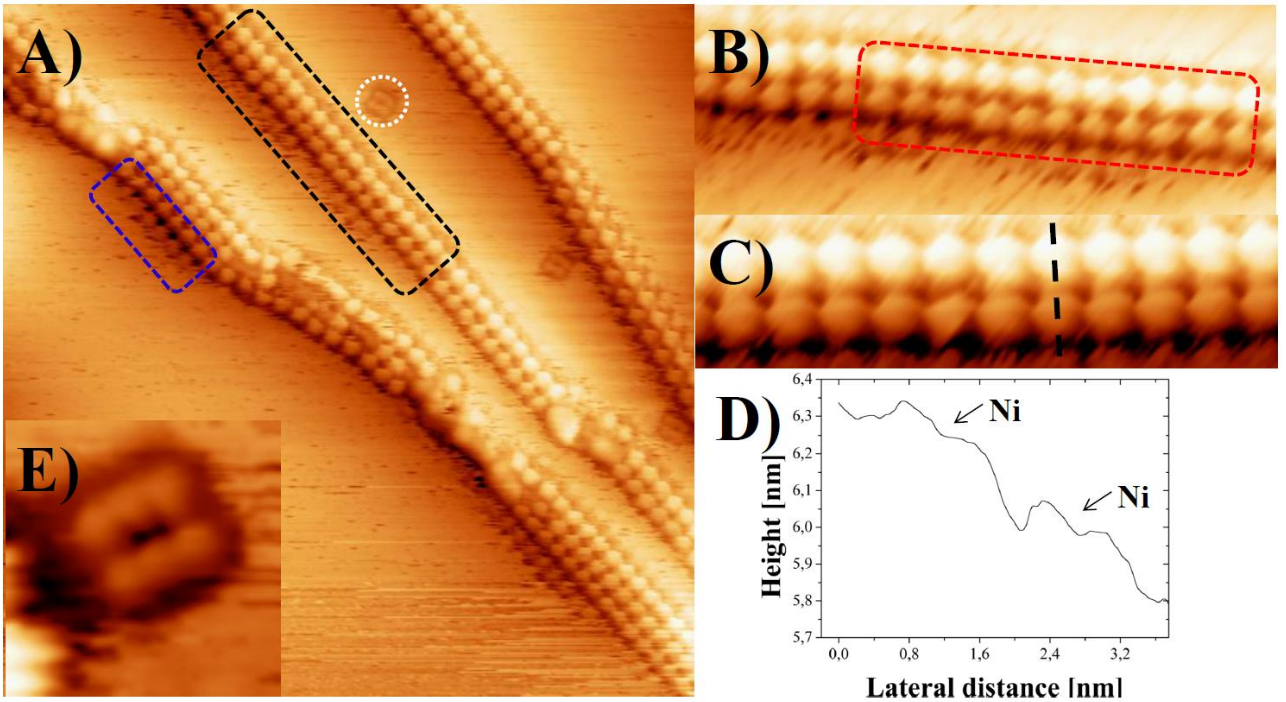

Figure 2. A) STM image (85x85 nm²) of the transition between disordered 1D nanochains to 2D self-assembly (VT=1.5 V and IT=0.6 nA) for a coverage of ~0.2ML. The nucleated molecules in the lower terraces are inside the dashed blue rectangles. In dashed circle, an example of TPP molecule locked at a surface defect. B) Zoom-in STM image of the dashed black rectangle (22x8 nm²) in (A) showing one of the lower terraces with molecule adsorption. C) Zoom-in STM image (15x4 nm²) of dashed red rectangle in (B) showing the regular pattern of the double atomic height row (VT=1.5 V and IT=0.3 nA). D) Line profile of the black line in (C). E) STM image (3x3 nm², VT=0.8 V and IT=0.5 nA) of unusual molecular occupancy at the middle of the terrace, attributed to adsorption on a defect or being a different molecule (possibly 2H-TPP).

By measuring the apparent length of the molecules parallel to the step edge, it is possible to correlate this measurement with the molecule orientation angle at the step edge. We perform this analysis by acquiring a line scan profile across the molecules at the step edge and measuring the distance between adjacent protrusions of NiTPP, at the same bias voltage, thus obtaining the molecular separation. We claim from the counting of different molecular separations (histogram shown in Figure 1 B) that our distribution is random. Although the molecular separation should vary from 1.2 to 1.8 nm, molecules packed either via its smallest dimension or via its diagonals, in the histogram it is also possible to see measurements lower than 1.2 nm and greater than 1.8 nm. This could be due to the superposition of molecules in the images or some molecules might be adsorbed on top of step defects, causing the over- or underestimation in the molecular separation distance. Since there is no prominent, well defined value in the histogram, we conclude that our molecular separation distribution can be assumed as uniform, meaning that molecules are randomly oriented across the step edges. When chemical elements such as carbon, sulphur or oxygen are present at a metallic surface, they tailor the properties of the step edges of the substrate and serve as anchoring sites for the molecules, but in our case XPS measurements show absence of impurities on the copper surface. Therefore, our proposed explanation is that NiTPP can diffuse on the surface until it finds the step edges which act as a trapping potential with an energy barrier higher than the energy associated with room temperature. This result differs from the one obtained by Rojas et al. [25] for the unmetallated tetraphenyl porphyrin (H2TPP) on Cu(111), where, at low coverage, the H2TPP does not present step decoration. On the other hand, different tetraphenyl porphyrins such as CoTPP also show step decoration on metallic substrates such as Au(111) and Ag(111) [14, 26], but on Cu(111) there are also molecules adsorbed in the middle of terraces at room temperature [27]. Therefore, not only the choice of substrate but also of metal center of the TPP influences the adsorption behavior of molecules, especially in the low coverage regime.

Transition between disordered one-dimensional and ordered two-dimensional adsorption

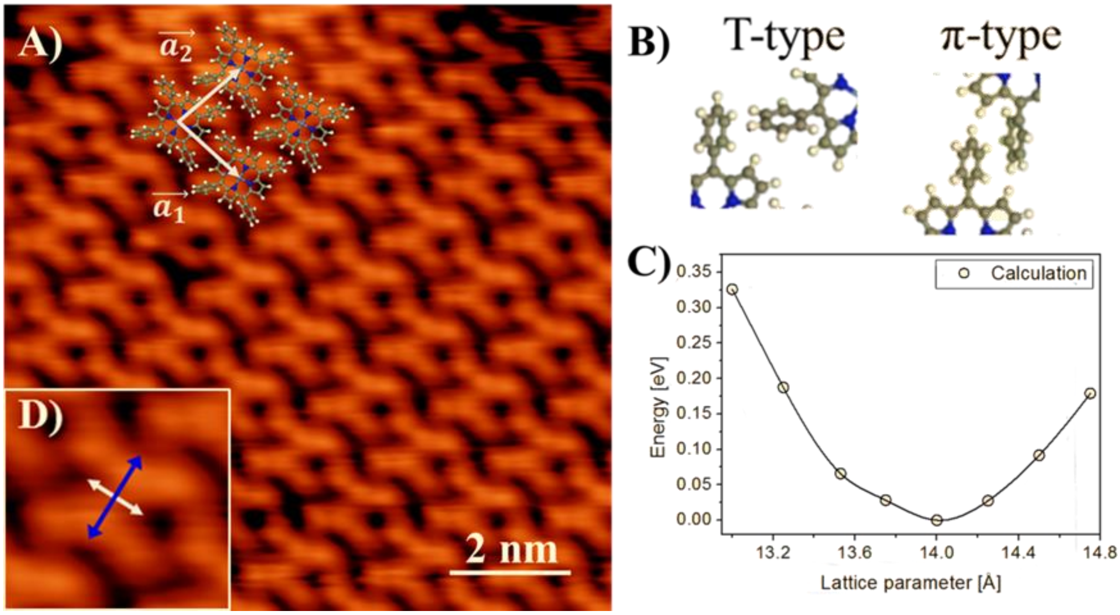

Figure 3. NiTPP on Cu(111) at monolayer coverage. A) STM image (10x10 nm²) showing the 2D closed-packed self-assembly of NiTPP on Cu(111) (VT=1.2 V and IT=0.3 nA). It is possible to see the 4-fold symmetry of the NiTPP. In the top left of the image there is a scheme of the unit cell with vectors a_1=(1.34±0.05)nm and a_2=(1.35±0.05)nm with their respective angle being (85±3)°. B) Representation of the T-type and π-type, when two phenyls of different molecules are either perpendicular or parallel to each other, respectively. C) Relative total energy of an isolated 2D array of free-standing NiTPP as a function of the intermolecular separation, taking the minimum energy as reference (the line is only a guide for eyes). D) NiTPP saddle-shape conformation shown in detail (2x2 nm²). The distances between opposite pyrroles (blue and white arrowed lines) are different.

The behavior of NiTPP transition to 2D nucleation was analyzed in our experiments. During the transition between 0.1 ML and 1.0 ML the nucleation of the NiTPP was found to start at the step edge. No free-islands of NiTPP were observed on the Cu(111) terraces during measurements. Other porphyrinic systems, such as the tetra butyl phenyl porphyrin (H2TBPP) on Cu(100) [28] present the formation of 2D islands in the middle of terraces at room temperature. For the NiTPP/Cu(111) system the molecular adsorption mechanism consists first of step edge decoration followed by the disordered 1D molecular chain starting to align with other NiTPP that adsorbs near these chains. When the terraces have diatomic height, it was observed that NiTPP prefers to nucleate on the step edge and create a double molecular chain, as indicated in Figure 2 C. In this case the random behavior of the distances between molecules is replaced by an ordered regime. The metal atom of the TPP molecule is indicated in Figure 2 D in the line profile of the double nanochain as a depression at its center. The nickel center is measured as a depression due to the lower tunneling probability in the center, because of the electronic filling of the dz² orbital as concluded by Lu and Hipps [15]. The average distance measured between molecules in these observed nanochains shows that they possess a periodic intermolecular distance of (1.35±0.03) nm. This implies that when there is a higher density of molecules, their interaction starts to guide molecules in a specific orientation, moving towards a regular assembly regime. Therefore, we conclude that the condition for orientation of molecules in the submonolayer coverage regime is that incoming molecules interact with the molecules at the step edge and this interaction orientates the molecules. By losing mobility of the reported mobile phase of NiTPP, more molecules begin to interact with the chain, thus forming a 2D closed packed arrangement. This behavior is shown in Figures 2 A and 2 B, for coverage of approximately 0.2 ML, with the nucleated molecules being visible near the step edges.

Although molecules were not observed to nucleate in islands in the middle of the terrace, single molecules were observed in these regions (see Figure 2 A). We attribute such behaviour to two possibilities: 1) A foreign molecule. Since we have used a commercial molecule source, they contain a small percentage of impurities. Some of these impurities might have been present at the time molecules were deposited. The unusual electronic corrugation shown in Figure 2E, where it is not possible to image the lobes, supports this idea. 2) It is a TPP molecule trapped in a terrace defect.

Two dimensional assembly and chirality.

The study now focuses on higher coverage, when intermolecular interaction plays a key role and the molecular self-assembling process occurs. Figure 3 A shows a typical high resolution STM image from a large ordered area on the surface when coverage range ~1 ML of NiTPP on Cu(111). The NiTPP assembles in an almost-square lattice, with unit cells of a_1=(1.35±0.04) nm by a_2=(1.34±0.04) nm and their relative angle being (85±3) degrees. This 2D behavior is similar to the formation on the NiTPP/Au(111) [16], and CuTPP/Cu(111) [29]. Differently from Teugels et al. [16], no parallelogram structure was found for this system, indicating that due to a higher reactivity of the substrate, molecular arrangements that require lower interaction between molecules and substrates are undermined.

In the diagram of the NiTPP in Figure 3 A, the main intermolecular interaction was depicted as being caused by the so called T-type interaction [17, 29, 30]. In the T-type interaction, shown in Figure 3 B, the C-H group of the phenyl structure interacts strongly and attractively with the center of the π-system of the phenyl structure of an adjacent NiTPP. Another possible intermolecular interaction would be the π-type interaction (Figure 3 (B)), where the phenyl structure from different molecules are parallel to each other, thus creating an overlap in the final molecular orbital. In the present study there is no evidence that π-type interactions are occurring.

In order to evaluate the energetic stability of isolated NiTPP molecules adsorbed on the Cu(111) surface in different sites and also the stability of the 2D array, we calculate the adsorption energy E_a, which can be written as,

$$E_a = E[Cu(111)] + E[NiTPP] - E[NiTPP/Cu(111)].$$

E[Cu(111)] and E[NiTPP] represents the total energies of the isolated components, the Cu(111) clean surface and the isolated NiTPP molecule, respectively, and E[NiTPP/Cu(111)] represents the total energy of the NiTPP/Cu(111) adsorbed system. According to the previous equation, positive values of E_a imply that the adsorption process is exothermic. In this work, considering the geometry of the Cu(111) surface, we investigated four adsorption sites for the isolated NiTPP molecule. All adsorption positions are identified with respect to Ni atom, as seen in Figure 4 E. The adsorption energy corresponding to those sites are summarized in Table I.

In our simulations the equilibrium geometry, as well as the vertical distortion of the phenyl-rings of an isolated NiTPP molecule, Fig. 4 A, are in agreement with the energetically most stable (S4) configuration obtained by Rush et al. [31]. Our results of E_a are close to those obtained by Brede et al. [29] who obtained an E_a of 3.4 eV for TPP on the Au(111) surface. We find an E_a of ~2.9 eV/molecule for a single molecule adsorbed on the Cu(111) and 3.5 eV/molecule for the 2D self-assembled array. Therefore, DFT calculations indicate that the formation of 2D array of NiTPP molecules on Cu(111) surface is exothermic (energetically favorable) with respect to the situation in which the molecules are isolated.

Table I. Calculated adsorption energy per molecule (E_a) and vertical equilibrium distance (h) in different adsorption sites in two configurations – single molecule and self-assembled array. Adsorption energies in eV, and the NiTPP-Cu(111) equilibrium vertical distance (h) in Å.

Single molecule	E_a (eV/molecule)	h (Å)
Top	2.95	4.03
Bridge	2.94	3.97
hollow-fcc	2.92	3.90
hollow-hcp	2.91	3.86
Self-assembled array		
hollow-fcc	3.53	3.94
hollow-hcp	3.52	3.96
Bridge	3.52	3.95
Top	3.40	3.91

Since E_a is quite insensitive to the adsorption site and taking into account the large molecule-surface separation (typical for weak van der Waals interactions), as it can be seen in Table I, NiTPP is not expected to be strongly bond to any special position on the clean Cu(111) surface. In this case, the NiTPP molecule is able to easily diffuse before it encounters other NiTPP molecules or is trapped in the vicinity of an extended defect (e.g. the edges), as indeed observed in the experiments. It is also worthwhile to evaluate separately the energy contribution of molecule-molecule interactions to the formation of 2D array. With this assumption, we calculate the total energy of a suspended 2D array of NiTPP as a function of the lattice vectors a_1 and a_2. Here, the Cu(111) surface potential has been turned off. As presented in Fig. 3 C, we find an energy minimum for a lateral distance (a_1 and a_2, depicted in Figure 4 C) of 1.4 nm, in agreement with the experimental results. From these results it is possible to conclude that molecular ordering in the monolayer range is mainly ruled by intermolecular interaction without a prominent influence from the substrate.

Our experiments reveal that the NiTPP (2D self-assembled) molecules exhibit a saddle-shape conformation. The hydrogen repulsion between phenyl and pyrroles is responsible for the conformation of the macrocycle of the porphyrin. As shown in Figure 3 D, this can be concluded from the different sizes between perpendicular opposed pyrroles. This difference is explained due to steric repulsion of the pyrroles by the phenyl rings that are rotated with respect to the TPP macrocycle. Opposed pyrroles are bent upwards (py-up in Figure 4 B) whereas perpendicular pyrroles, downwards (py-dw in Figure 4B).

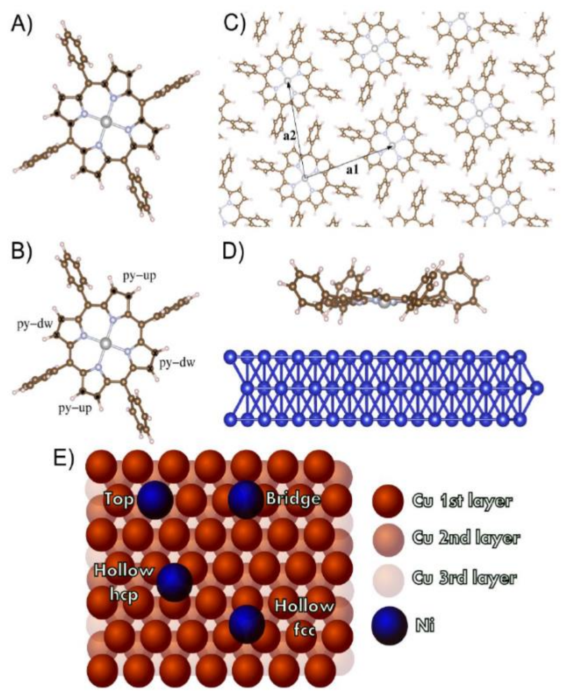

Figure 4. Structural models of isolated NiTPP molecule (A) and (B). The relative upward (represented as a dot) and downward (represented as a cross) displacements of C atoms, of the phenyl rings. C) and D) shows the structural model of the NiTPP/Cu(111) 2D array. E) Representation of the Nickel atom of the NiTPP for different adsorption positions.

The molecule conformation upon its interaction with solid surfaces has been the subject of several studies [17, 29, 32]. Our calculated equilibrium geometries, for the 2D arrays of NiTPP molecules, support the experimentally observed saddle-shape, as depicted in Figure 4 B. Such saddle conformation can be measured by the vertical displacement of the edge carbon atoms of the pyrrole rings (ΔZpy) (Fig 4 B). In this case, we find (i) ΔZpy of about 0.125 nm for the isolated 2D array, while (ii) at the equilibrium geometry on the Cu(111) surface ΔZpy reduces to

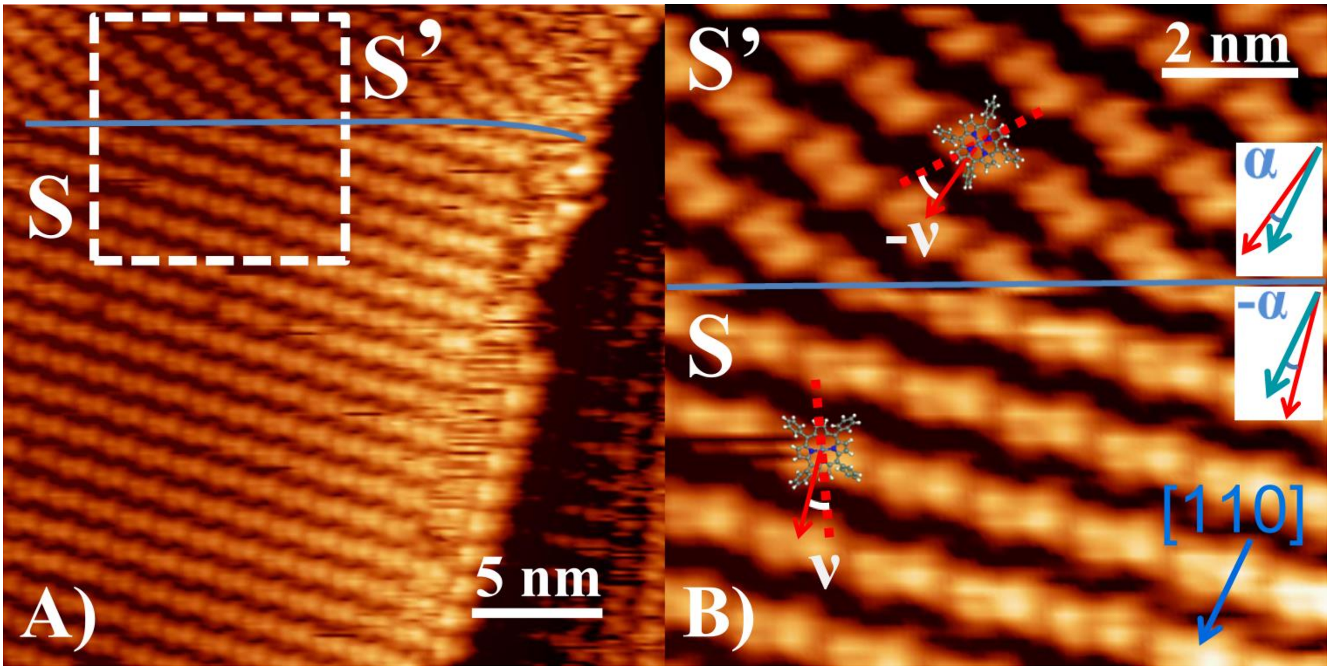

Figure 5. A) Large area STM image (25x25 nm²) (VT=1.2 V and IT=0.1 nA) showing the S and the S' domains in which NiTPP assembles. B) Small STM image (9x9 nm²) of the dashed area in figure A. It is possible to resolve both existing domains and compare one of their vector lattice with the gray arrow, representing one of the [110] main directions in Cu(111). The angle formed is α=(10±2)°, while the angle formed by one of the main axis of the NiTPP to the lattice vectors of the superstructure is ν=(25±2)°. Coverage of surface is ~ 1ML.

0.095 nm. Shortly, for 2D array of NiTPP molecules, the saddle configuration is defined by the molecule-molecule ("T-shape") interaction, whereas upon its interaction with the surface, the saddle conformation will be reduced. The possibility of the porphyrins being in the saddle or ruffled configuration has been treated in literature [33, 34].

In addition to the reduction of the saddle shape conformation, as depicted in Fig. 4 D, there is a vertical displacement of the phenyl rings of NiTPP, due to the steric (repulsive) interaction with the Cu(111) surface. By comparing the total energies of the deformed molecule and the free (isolated and fully relaxed) molecule, we can estimate the energy cost to deform the phenyl rings of NiTPP (ΔE_{deform}), upon its interaction with the surface. We find an energy ΔE_{deform} of 0.2 and 0.3 eV for a single molecule and 2D self-assembled array configuration, respectively. The latter result is somewhat expected, since there are additional NiTPP distortions due to the molecule-molecule (lateral) interactions.

Experimentally, we observe chiral domains in the self-assembled NiTPP, denoted S and S'. Figure 5 A displays a large area STM image with the chiral domains shown. S and S' domains were found to be rotated by α=(10±2)° from the [110] direction of Cu(111) crystal. The explanation for an achiral molecule to form a chiral superstructure, as discussed by Donovan et al [18], lies on the existence of the T-type interaction between phenyls. This interaction produces a tilt of the molecule so that one of the axes of NiTPP, formed by line connecting opposed nitrogen atoms has a relative angle with respect to one of its unit cell vectors. The tilt angle was calculated to be ν=(25±2)°, as shown in Figure 5 B.

XPS analysis of NiTPP/Cu(111).

We compare the monolayer and multilayer XPS signals to analyse the interaction of Cu(111) with the molecules. Figure 6 presents a survey XPS scan in both conditions.

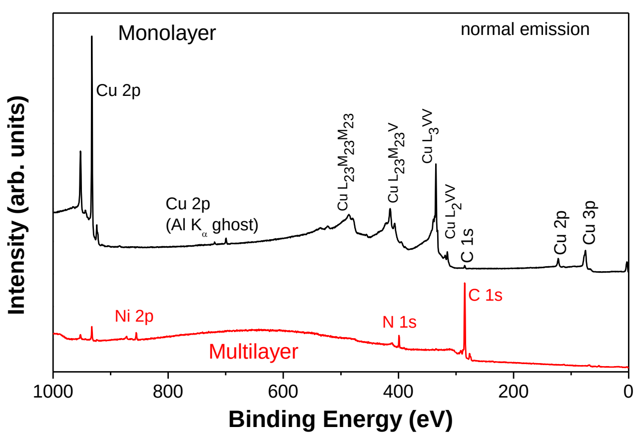

Figure 6. XPS Spectra for different NiTPP coverage. Approximately 1 ML of NiTPP is presented in black and 8 ML of NiTPP is presented in red. By the attenuation of the Cu $2p_{3/2}$ core line it was possible to estimate this coverage.

The multilayer coverage was calculated as being 8 ML by the attenuation of the Cu $2p_{3/2}$ signal [35]. The energy positions for each peak were determined using a standard fitting procedure considering Shirley type background and Voigt functions (not shown here). The multilayer signal of Ni $2p_{3/2}$ and C 1s core level positions are in good agreement with data reported in literature [36]. A chemical shift of 2.3 eV for the Ni $2p_{3/2}$ core line is observed for the monolayer configuration on Cu(111) when compared to NiTPP/Au(111) [13]. This corroborates the differences in the strength of the interaction to the substrate.

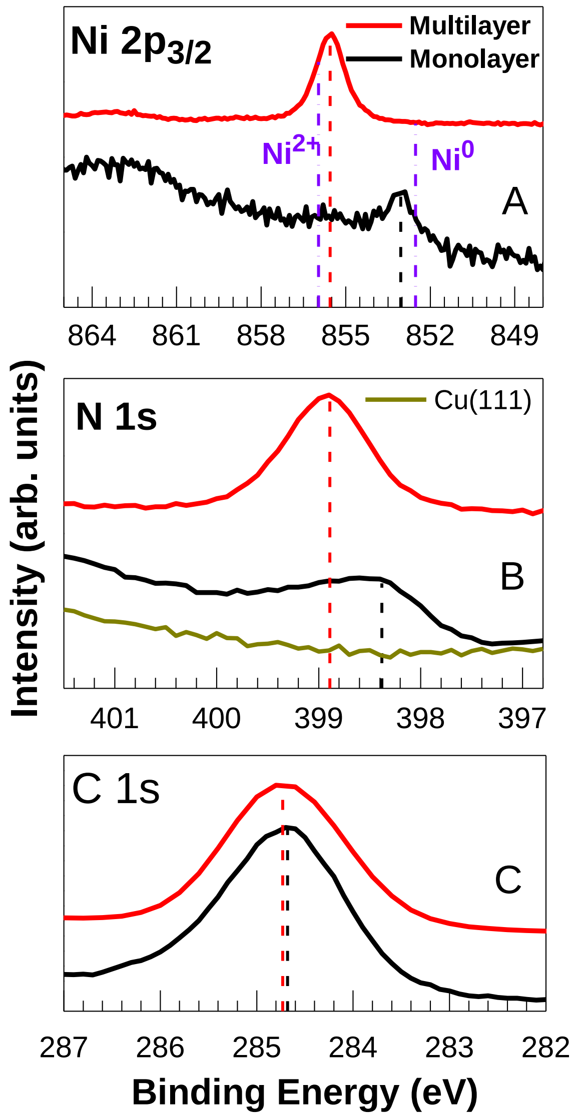

Figure 7. XPS spectra for different chemical elements in NiTPP for monolayer (black curves) and multilayer (red curves) coverage. A) Spectra of Ni 2p, showing a chemical shift of 2.5 eV. The violet dash-dotted lines represent the peaks of both Ni^0 and Ni^{2+} on Cu(111) [38], as a reference. B) Spectra of N 1s showing a chemical shift of 0.5 eV. For comparison, the bare Cu(111) spectrum is plotted as a green solid line, since the Cu LMM auger lines overlap in this region. C) Spectra of C 1s showing a chemical shift lower than 0.1 eV. Nickel is the atom that more strongly binds to the Cu(111) surface.

High resolution XPS from core-levels of the NiTPP chemical elements revealed different chemical shifts between the monolayer and the multilayer regime. The XPS spectra for the Ni $2p_{3/2}$ exhibits peaks centered in energies of 852.9 eV and 855.5 eV, respectively in the monolayer and the multilayer coverage, which represents a shift of 2.6 eV (Figure 7 A). The N 1s peak exhibits a chemical shift of 0.5 eV in the multilayer regime (Figure 7 B), while the C 1s signal shows a chemical shift of less than 0.1 eV between the same layered systems (Figure 7 C), both towards higher binding energies. The shifts observed for the C1s and N 1s are in accordance with the change in the interface of the molecules, from monolayer to multilayer, with similar shifts being observed in other porphyrinic systems [37].

The Ni $2p_{3/2}$ signal of the monolayer exhibits a smaller and broader feature at the same position of the multilayer case. Due the low signal to noise ratio, it is difficult to confirm that it is a component similar to the multilayer case; however the energy position is the same. Since the monolayer was calculated due to attenuation of the substrate and corroborated via STM images, some areas of the sample should have more than one monolayer, therefore could explain the existence of such peak.
For the monolayer regime, the position of the Ni $2p_{3/2}$ peak is 852.5 eV, a value closer to Ni^0 [38] and in the multilayer, 856.0 eV, comparable to the Ni^{+2} state founded in NiO_x [38]. The Ni^{+2} value is expected in the multilayer of NiTPP due to the coordination state of Ni in the molecule demonstrating a negligible influence of the substrate in the electronic or magnetic properties of the molecule. However, a more interesting possibility could be speculated in the monolayer regime where the null-like oxidation state could open a possibility to change the electronic or magnetic properties of the molecule for example stabilizing a new magnetic behavior, which could be induced by a charge transferring mechanism similarly to the magnetic switching induced by NH_3 adsorption on NiTPP [10] or in the case of thiol adsorption on Au nanoparticles [39]. Similar XPS shifts are reported in the literature for other metallic porphyrins, where the origin is attributed to several effects such as charge transfer, polarization screening and final state effects [39].

In order to get a more complete picture of the electronic interaction between the NiTPP molecule and the Cu(111) surface, initially we examine the adsorption of a Ni adatom on the Cu(111) surface, Ni/Cu(111). Different from the NiTPP/Cu(111) system, in Ni/Cu(111) we have the formation of the chemical bonds between the adatoms and the Cu(111) surface. The strength of Ni-Cu(111) interaction can be quantified by the calculation of the adsorption energy (Ea), as we have done for NiTPP on Cu(111). Here, we have considered (i) the same Ni coverage as we have used in the array geometry of NiTPP/Cu(111) system, namely around 3.1% of a monolayer, and (ii) the following adsorption sites on the Cu(111) surface, hollow-fcc, hollow-hcp, and bridge. We find Ea of 3.38, 3.38 and 3.35 eV/atom, respectively.

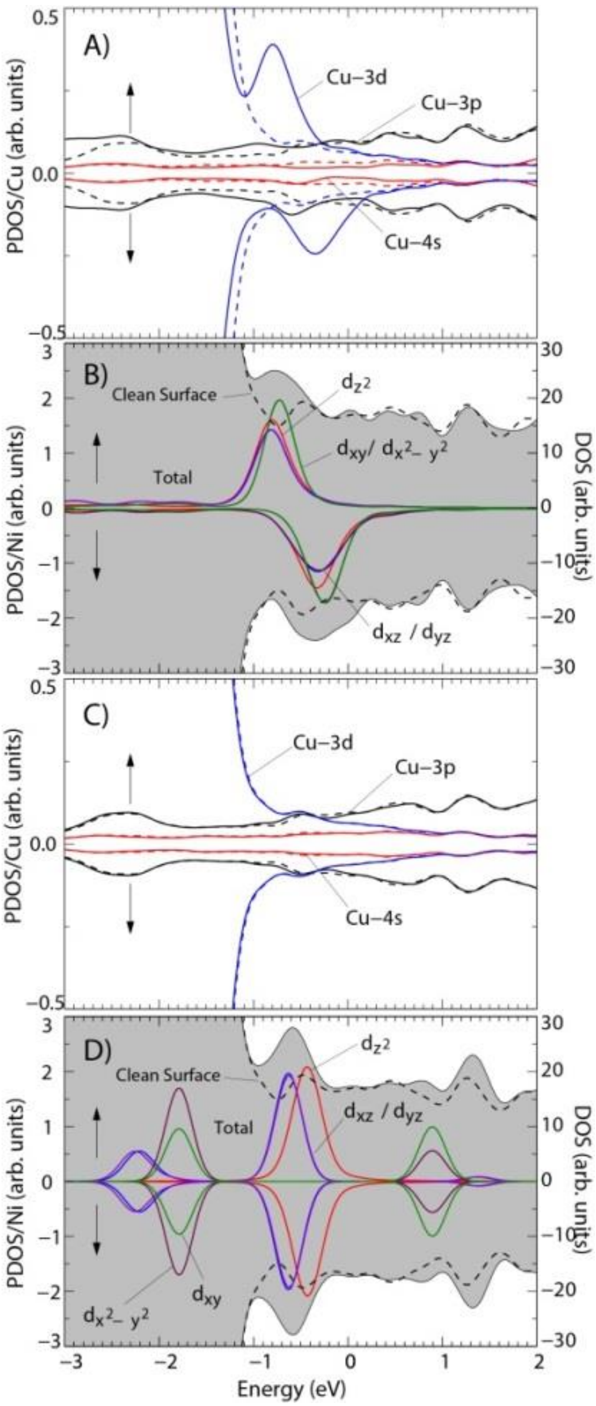

Figure 8. Total density of states (DOS) and the projected DOS (PDOS) of the surface Cu atoms (A), and Ni-3d orbitals (B) of the Ni/Cu(111) system. (C) PDOS of the surface Cu and, (D) total DOS, and PDOS of Ni-3d orbitals, of the NiTPP/Cu(111). Dashed lines indicate the DOS and PDOS of the clean Cu(111) surface.

In Fig. 8A, we present the projected density of states (PDOS) of the surface Cu atoms nearest neighbor to the Ni adatom in the hollow-fcc site (solid lines), and the PDOS of the same surface Cu atoms of the clean surface (dashed lines). We observe that the spin-up and spin-down components of the occupied Cu-3d orbitals, within EF – 1 eV, present an energy (spin) splitting of around 0.46 eV induced by the Ni adatoms. The Ni adatom on the hollow-fcc site presents a net magnetic moment of 0.73 μB, mostly ruled by the partial occupation of the Ni-3d orbitals, as shown in Fig. 8B. For the Ni adsorption on the hollow-hcp and bridge sites we find 0.70 and 0.66 μB, respectively. These results of net magnetic moment are in agreement with the previous studies performed by Lazarovits et al. [40]. The spin-up and spin-down components of the Ni-3d orbitals, at EF – 1 eV, present an energy splitting of around 0.5 eV [Fig. 8B], being resonant with the one of surface Cu-3d orbitals, indicating a strong hybridization between the 3d orbitals of Ni adatom and the surface Cu atoms. In contrast, the electronic structure of the surface Cu states are weakly perturbed upon the adsorption of NiTPP molecules. Indeed, there no changes on the PDOS of the Cu-3d orbitals of NiTPP/Cu(111) and the Cu(111) clean surface, indicated by solid and dashed lines in Fig. 8C, supporting the absence of chemical interaction between the NiTPP molecule and the Cu(111) surface. Figure 8 depicts the total density of states (DOS) of the NiTPP/Cu(111) surface, and the projected DOS (PDOS) of Ni 3d orbitals, for the array geometry of NiTPP molecules adsorbed on the hollow-fcc sites of Cu(111). In the same diagram (dashed lines), we present the DOS of the clean Cu(111) surface. In general, the electronic states of the surface are weakly perturbed by NiTPP adsorption. We find that the highest occupied Ni 3d$_{z^2}$, 3d$_{xz}$ and 3d$_{yz}$ states lie within an energy interval of E_F – 1 eV, whereas the lowest unoccupied states (for E_F +1 eV) are composed by Ni-3d$_{xy}$ and 3d$_{x^2-y^2}$ orbitals. The occupied 3d$_{xy}$ and 3d$_{x^2-y^2}$ orbitals are at EF – 2 eV. Here, different from the Ni/Cu(111) system, the spin-up and spin-down components of the occupied Ni-3d orbitals do not exhibits any energy (spin) splitting. Such PDOS picture is the same for the other NiTPP/Cu(111) configurations, namely NiTPP adsorbed on the hollow-hcp, top and bridge sites. Those findings corroborate the lack of differences between calculated E_a for different adsorption sites. In contrast, for the CoTPP/Ag(111) system, the authors verified that PDOS shows a clear dependence with the CoTPP adsorption site [17]. In addition, (i) there is a downshift of 0.5 and 0.4 eV of the Ni-3d$_{z^2}$ and 3d$_{xz}$ orbitals, respectively, with respect to the energy positions of an isolated NiTPP molecule (indicated by dashed lines), and (ii) the Ni-3d$_{z^2}$ orbital exhibits a slight increase on the PDOS energy distribution width, due to its interaction with the Cu(111) surface. Indeed, based on the Bader charge density analysis [41], we find a small net charge transfer of 0.06e between the molecule and the Cu(111), preserving the low-spin configuration of the NiTPP molecule.

Conclusion

In this coverage study of the NiTPP/Cu(111) by STM, molecular step edge decoration was observed with random orientations for submonolayer coverage. We envisage applying this behavior towards the growth of NiTPP on vicinal surfaces for 1D oriented wires at room temperature. Whenever more molecules nucleate in the system, the molecules at the step edge start to orientate in the same relative position. Such orientation behavior was corroborated by STM measurements not only for the single step edges but also in regions where step edges have 2-atoms height. For higher coverage, molecules self-assemble in a 2D square-like array, where the most important contribution is due to phenyl-

phenyl interaction, as corroborated by DFT. The self-assembled arrays form chiral structures, due to the same phenyl-phenyl interaction in the so called T-type interaction. NiTPP exhibits a saddle-shape conformation, as observed by STM and demonstrated via DFT. XPS results of Ni $2p_{3/2}$ showed a chemical shift between mono- and multilayers of NiTPP. All the theoretical and indirect evidences exploring the molecules in the monolayer regime tend to reject the charge transfer mechanism between the Ni center atom and the Cu substrate.

Acknowledgment

This work was supported by FAPESP, CNPq, LNLS and CAPES from Brazil. S.F. gratefully acknowledges FAPESP studentship 2012/16860-8 and 2013/04855-0. R.G.A.V. thanks funding provided by the FAPESP grant 2011/19564-6 and 2014/10294-4. MJP thanks funding provided by the FAPESP grant 2011/12566-3. This work used computational facilities provided on the Blue Gene/P supercomputer supported by the Research Computing Support Group (Rice University) and Laboratório de Computação Científica Avançada (Universidade de São Paulo).

REFERENCES

(1) Barth, J. V.; Costantini, G.; Kern, K.; *Nature* 2005, 437, 671–679
(2) Castonguay, M.; Roy, J.-R.; Rochefort, A.; McBreen, P. H. ; *Journal of the American Chemical Society* 2000, 122, 518–524.
(3) Oliver, I. T.; Rawlinson, W. A. ; *Biochemical Journal* 1955, 61, 641–646.
(4) Forrest, S. R. ; *Chemical Reviews* 1997, 97, 1793–1896.
(5) Koch, N. Organic Electronic Devices and Their Functional Interfaces. *ChemPhysChem* 2007, 8, 1438–1455.
(6) A. Shelnutt, J.; Song, X.-Z.; Ma, J.-G.; Jia, S.-L.; Jentzen, W.; J. Medforth, C.; J. Medforth, C.; Nonplanar Porphyrins and Their Significance in Proteins. *Chemical Society Reviews* 1998, 27, 31.
(7) Haworth, P.; Watson, J. L.; Arntzen, C. J.; *Biochimica et Biophysica Acta (BBA) - Bioenergetics* 1983, 724, 151–158.
(8) Voet, D.; Wiley: New York, 1990.
(9) Wäckerlin, C.; Chylarecka, D.; Kleibert, A.; Müller, K.; Iacovita, C.; Nolting, F.; Jung, T. A.; Ballav, N.; *Nature Communications*2010, 1, 1–7.
(10) Wäckerlin, C.; Tarafder, K.; Girovsky, J.; Nowakowski, J.; Hählen, T.; Shchyrba, A.; Siewert, D.; Kleibert, A.; Nolting, F.; Oppeneer, P. M.; et al. ;*Angewandte Chemie International Edition* 2013, 52, 4568–4571.
(11) Flechtner, K.; Kretschmann, A.; Bradshaw, L. R.; Walz, M.-M.; Steinrück, H.-P.; Gottfried, J. M; *The Journal of Physical Chemistry C* 2007, 111, 5821–5824.
(12) Auwärter, W.; Weber-Bargioni, A.; Brink, S.; Riemann, A.; Schiffrin, A.; Ruben, M.; Barth, J. V. ; *ChemPhysChem* 2007, 8, 250–254.
(13) Chen, M.; Feng, X.; Zhang, L.; Ju, H.; Xu, Q.; Zhu, J.; Gottfried, J. M.; Ibrahim, K.; Qian, H.; Wang, J.; *The Journal of Physical Chemistry C* 2010, 114, 9908–9916.
(14) Yang, Z.-Y.; Durkan, C. ; *Surface Science* 2010, 604, 660–665.
(15) Lu, X.; Hipps, K. W.; *The Journal of Physical Chemistry B* 1997, 101, 5391–5396.
(16) Teugels, L. G.; Avila-Bront, L. G.; Sibener, S. J.; *The Journal of Physical Chemistry C* 2011, 115, 2826–2834.
(17) Auwärter, W.; Seufert, K.; Klappenberger, F.; Reichert, J.; Weber-Bargioni, A.; Verdini, A.; Cvetko, D.; Dell'Angela, M.; Floreano, L.; Cossaro, A.; et al.; *Physical Review B* 2010, 81.
(18) Donovan, P.; Robin, A.; Dyer, M. S.; Persson, M.; Raval, R. ; *Chemistry - A European Journal* 2010, 16, 11641–11652.
(19) Horcas, I.; Fernández, R.; Gómez-Rodríguez, J. M.; Colchero, J.; Gómez-Herrero, J.; Baro, A. M.; *Review of Scientific Instruments* 2007, 78, 013705.
(20) Giannozzi, P.; Baroni, S.; Bonini, N.; Calandra, M.; Car, R.; Cavazzoni, C.; Ceresoli, D.; Chiarotti, G. L.; Cococcioni, M.; Dabo, I.; et al.; Journal of Physics*: Condensed Matter* 2009, 21, 395502.
(21) Dion, M.; Rydberg, H.; Schröder, E.; Langreth, D. C.; Lundqvist, B. I.; *Physical Review Letters* 2004, 92.
(22) Thonhauser, T.; Cooper, V. R.; Li, S.; Puzder, A.; Hyldgaard, P.; Langreth, D. C.; *Physical Review B* 2007, 76.
(23) Román-Pérez, G.; Soler, J.; *Physical Review Letters* 2009, 103.
(24) Ehrlich, G.; Hudda, F. G. J.; *Chem. Phys.* 1966, 44, 1039−1049.
(25) Rojas, G.; Chen, X.; Bravo, C.; Kim, J.-H.; Kim, J.-S.; Xiao, J.; Dowben, P. A.; Gao, Y.; Zeng, X. C.; Choe, W.; et al; *The Journal of Physical Chemistry C* 2010, 114, 9408–9415.
(26) Buchner, F.; Kellner, I.; Hieringer, W.; Görling, A.; Steinrück, H.-P.; Marbach, H.; *Physical Chemistry Chemical Physics* 2010, 12, 13082.
(27) Buchner, F.; Xiao, J.; Zillner, E.; Chen, M.; Röckert, M.; Ditze, S.; Stark, M.; Steinrück, H.-P.; Gottfried, J. M.; Marbach, H.; *The Journal of Physical Chemistry C* 2011, 115, 24172–24177.
(28) Kamikado, T.; Sekiguchi, T.; Yokoyama, S.; Wakayama, Y.; Mashiko, S.; *Thin Solid Films* 2006, 499, 329–332.
(29) Brede, J.; Linares, M.; Kuck, S.; Schwöbel, J.; Scarfato, A.; Chang, S.-H.; Hoffmann, G.; Wiesendanger, R.; Lensen, R.; Kouwer, P. H. J.; et al. *Nanotechnology* 2009, 20, 275602.
(30) Bludský, O.; Rubeš, M.; Soldán, P.; Nachtigall, P. *The Journal of Chemical Physics* 2008, 128, 114102.
(31) Rush, T. S.; Kozlowski, P. M.; Piffat, C. A.; Kumble, R.; Zgierski, M. Z.; Spiro, T. G. *The Journal of Physical Chemistry B* 2000, 104, 5020–5034.
(32) Jung, T. A.; Schlittler, R. R.; Gimzewski, J. K.; *Nature* 1997, 386, 696–698.
(33) Fleischer, E. B.; Miller, C. K.; Webb, L. E.; *Journal of the American Chemical Society* 1964, 86, 2342–2347.
(34) Kosal, M. E.; Suslick, K. S. *Journal of Solid State Chemistry* 2000, 152, 87–98.
(35) Briggs, D.; Seah, M.P.; Practical Surface Analysis by Auger and X-ray Photoelectron Spectroscopy, 1st ed.; Wiley: Chichester, 1983.
(36) Karweik, D. H.; Winograd, N.; *Inorganic Chemistry* 1976, 15, 2336–2342.
(37) Bai, Y.; Sekita, M.; Schmid, M.; Bischof, T.; Steinrück, H.-P.; Gottfried, J. M.; *Physical Chemistry Chemical Physics* 2010, 12, 4336.
(38) Domnick, R.; Held, G.; Steinrück, H.-P.; *Surface Science* 2002, 516, 95–102.
(39) Yamamoto, Y.; Miura, T.; Suzuki, M.; Kawamura, N.; Miyagawa, H.; Nakamura, T.; Kobayashi, K.; Teranishi, T.; Hori, H; *Phys. Rev. Lett*. 2004, 93, 116801.
(40) Lazarovits, B; Szunyogh, L; Weinberger, P. *Phys. Rev. B* 2006, 73, 045430.
(41) Henkelman, G.; Arnaldsson, A.; Jónsson, H. *Science* 2006, 36, 354–360.

Table of Contents